





**UNIVERSIDAD DE INVESTIGACIÓN DE TECNOLOGÍA  
EXPERIMENTAL YACHAY**

**Escuela de Ciencias Físicas y Nanotecnología**

**TÍTULO: Construction of an electromagnet for the  
development of a vibrating sample magnetometer**

Trabajo de integración curricular presentado como requisito para la  
obtención del título de Ingeniero en Nanotecnología.

**Autor:**

Piedra Marin Luis Eduardo

**Tutor:**

Werner Brämer-Escamilla, PhD

Urcuquí, noviembre 2020

Urcuquí, 10 de noviembre de 2020

**SECRETARÍA GENERAL**  
**(Vicerrectorado Académico/Cancillería)**  
**ESCUELA DE CIENCIAS FÍSICAS Y NANOTECNOLOGÍA**  
**CARRERA DE NANOTECNOLOGÍA**  
**ACTA DE DEFENSA No. UITEY-PHY-2020-00020-AD**

A los 10 días del mes de noviembre de 2020, a las 10:30 horas, de manera virtual mediante videoconferencia, y ante el Tribunal Calificador, integrado por los docentes:

<b>Presidente Tribunal de Defensa</b>	Dr. MEDINA DAGGER, ERNESTO ANTONIO , Ph.D.
<b>Miembro No Tutor</b>	Dra. PERALTA ARCIA, MAYRA ALEJANDRA DE JESUS , Ph.D.
<b>Tutor</b>	Dr. BRAMER ESCAMILLA , WERNER , Ph.D.

El(la) señor(ita) estudiante **PIEDRA MARIN, LUIS EDUARDO**, con cédula de identidad No. **0926102450**, de la **ESCUELA DE CIENCIAS FÍSICAS Y NANOTECNOLOGÍA**, de la Carrera de **NANOTECNOLOGÍA**, aprobada por el Consejo de Educación Superior (CES), mediante Resolución **RPC-SO-13-No.156-2015**, realiza a través de videoconferencia, la sustentación de su trabajo de titulación denominado: **CONSTRUCTION OF AN ELECTROMAGNET FOR THE DEVELOPMENT OF A VIBRATING SAMPLE MAGNETOMETER**, previa a la obtención del título de **INGENIERO/A EN NANOTECNOLOGÍA**.

El citado trabajo de titulación, fue debidamente aprobado por el(los) docente(s):

<b>Tutor</b>	Dr. BRAMER ESCAMILLA , WERNER , Ph.D.
--------------	---------------------------------------

Y recibió las observaciones de los otros miembros del Tribunal Calificador, las mismas que han sido incorporadas por el(la) estudiante.

Previamente cumplidos los requisitos legales y reglamentarios, el trabajo de titulación fue sustentado por el(la) estudiante y examinado por los miembros del Tribunal Calificador. Escuchada la sustentación del trabajo de titulación a través de videoconferencia, que integró la exposición de el(la) estudiante sobre el contenido de la misma y las preguntas formuladas por los miembros del Tribunal, se califica la sustentación del trabajo de titulación con las siguientes calificaciones:

Tipo	Docente	Calificación
Tutor	Dr. BRAMER ESCAMILLA , WERNER , Ph.D.	10,0
Presidente Tribunal De Defensa	Dr. MEDINA DAGGER, ERNESTO ANTONIO , Ph.D.	8,8
Miembro Tribunal De Defensa	Dra. PERALTA ARCIA, MAYRA ALEJANDRA DE JESUS , Ph.D.	9,1

Lo que da un promedio de: **9.3 (Nueve punto Tres)**, sobre 10 (diez), equivalente a: **APROBADO**

Para constancia de lo actuado, firman los miembros del Tribunal Calificador, el/la estudiante y el/la secretario ad-hoc.

Certifico que *en cumplimiento del Decreto Ejecutivo 1017 de 16 de marzo de 2020, la defensa de trabajo de titulación (o examen de grado modalidad teórico práctica) se realizó vía virtual, por lo que las firmas de los miembros del Tribunal de Defensa de Grado, constan en forma digital.*

PIEDRA MARIN, LUIS EDUARDO  
**Estudiante**



Dr. MEDINA DAGGER, ERNESTO ANTONIO , Ph.D.  
**Presidente Tribunal de Defensa**



Firmado digitalmente por:  
**ERNESTO ANTONIO  
 MEDINA DAGGER**

Dr. BRAMER ESCAMILLA , WERNER , Ph.D.  
**Tutor**



Firmado electrónicamente por:  
**WERNER  
BRAMER**

Dra. PERALTA ARCIA, MAYRA ALEJANDRA DE JESUS , Ph.D.  
**Miembro No Tutor**



Firmado electrónicamente por:  
**MAYRA ALEJANDRA DE  
JESUS PERALTA ARCIA**

VILLARRUEL ALMEIDA, SANDRA VERONICA  
**Secretario Ad-hoc**



Firmado electrónicamente por:  
**SANDRA VERONICA  
VILLARRUEL  
ALMEIDA**

## AUTORÍA

Yo, **Luis Eduardo Piedra Marin**, con cédula de identidad 0926102450, declaro que las ideas, juicios, valoraciones, interpretaciones, consultas bibliográficas, definiciones y conceptualizaciones expuestas en el presente trabajo; así cómo, los procedimientos y herramientas utilizadas en la investigación, son de absoluta responsabilidad de el/la autora (a) del trabajo de integración curricular. Así mismo, me acojo a los reglamentos internos de la Universidad de Investigación de Tecnología Experimental Yachay.

Urququí, noviembre 2020.



---

Luis Eduardo Piedra Marin

CI: 0926102450

## AUTORIZACIÓN DE PUBLICACIÓN

Yo, **Luis Eduardo Piedra Marin**, con cédula de identidad 0926102450, cedo a la Universidad de Investigación de Tecnología Experimental Yachay, los derechos de publicación de la presente obra, sin que deba haber un reconocimiento económico por este concepto. Declaro además que el texto del presente trabajo de titulación no podrá ser cedido a ninguna empresa editorial para su publicación u otros fines, sin contar previamente con la autorización escrita de la Universidad.

Asimismo, autorizo a la Universidad que realice la digitalización y publicación de este trabajo de integración curricular en el repositorio virtual, de conformidad a lo dispuesto en el Art. 144 de la Ley Orgánica de Educación Superior

Urququí, noviembre 2020.



---

Luis Eduardo Piedra Marin

CI: 0926102450



## **Dedication**

This degree work is dedicated to my parents Luis Eduardo Piedra Aguirre and Jennifer Karim Marin Avalos, to my brother Isaac Francisco Piedra Marin, and lastly to my grandmother Rosita Elvira Avalos Soto who unfortunately passed away during the process of developing this degree work.

Luis Eduardo Piedra Marin

## **Acknowledgements**

First, I would like to give special thanks to my advisor Werner Bramer for the encouragement and advice that is greatly appreciated. Secondly, I want to thank my parents and family that support me during my whole career at Yachay Tech University. Finally, I would like to thank the School of Physical Science and Nanotechnology for all the knowledge and opportunities that gave to all students to become great professionals.

Luis Eduardo Piedra Marin



## Resumen

El magnetómetro de muestra vibrante (VSM) es una máquina que mide el momento magnético y la susceptibilidad magnética de los materiales cuando vibran perpendicularmente a un campo magnético uniforme. Los VSM comerciales son muy costosos y los más simples solo producen campos magnéticos de hasta 0.7 Tesla. Sin embargo, todavía requieren grandes imanes para el núcleo del electroimán con su enorme fuente de alimentación y su sistema de refrigeración. Este proyecto de tesis presenta el diseño, construcción y calibración de un electroimán de bajo costo con su fuente de alimentación que proporciona valores de campo magnético de hasta 0.5 Tesla. Este electroimán cumple con los requisitos para desarrollar un VSM para un laboratorio de pregrado. La caracterización de materiales magnéticos blandos exige un campo magnético VSM adecuado que se genera a partir del electroimán y su fuente de alimentación. El resultado final de este proyecto de tesis muestra las diferentes configuraciones de medición para producir diferentes valores de campo magnético. Estas configuraciones de medición se dividen en corriente ascendente y corriente descendente. La configuración de corriente ascendente muestra valores de 36 mT a 496 mT. La configuración de corriente descendente muestra valores de 557 mT a 32 mT. El panel frontal de la fuente de alimentación tiene un interruptor selector que tiene 18 sujetadores de latón de hoja de papel conectados a 18 salidas de nueve transformadores. Por lo tanto, hay un total de 36 valores de campo magnético (18 para corriente ascendente y 18 para corriente descendente) para la medición de la magnetización del material de muestra.

**Palabras clave:** VSM, electroimán, fuente de alimentación, Tesla, campo magnético, materiales magnéticos blandos.

## Abstract

The Vibrating Sample Magnetometer (VSM) is a machine that measures the magnetic moment and magnetic susceptibility of materials when they are vibrating perpendicular to a uniform magnetic field. Commercial VSM are highly costly and the simplest ones only produce magnetic fields up to 0.7 Tesla. However, they still require big magnets for the electromagnet core with its huge power supply and their refrigeration system. This thesis project presents the design, construction and calibration of a low cost electromagnet with its power supply that provides values of magnetic field up to 0.5 Tesla. This electromagnet fulfills the requirements to develop a VSM for an undergraduate laboratory. The characterization of soft magnetic materials demands an adequate VSM magnetic field that is generated from the electromagnet and its power supply. The final result of this thesis project shows the different configurations of measurement to produce different values of magnetic field. These configurations of measurement are divided into up current and down current. The up current configuration shows values from 36 mT to 496 mT. The down current configuration shows values from 557 mT to 32 mT. The front panel of the power supply has a selector switch which has 18 paper sheet brass fasteners connected to 18 output lines from nine transformers. Thus, there is a total of 36 values of magnetic field (18 for up current and 18 for down current) for the magnetization measurement of the sample material.

**Keywords:** VSM, electromagnet, power supply, Tesla, magnetic field, soft magnetic materials.



# Contents

<b>List of Figures</b>	<b>viii</b>
<b>List of Tables</b>	<b>x</b>
<b>List of Papers</b>	<b>xi</b>
<b>1 Introduction</b>	<b>1</b>
1.1 Problem Statement . . . . .	2
1.2 General and Specific Objectives . . . . .	2
<b>2 Theoretical background</b>	<b>3</b>
2.1 Vibrating Sample Magnetometer . . . . .	6
2.1.1 VSM working principle . . . . .	7
2.2 Detection Coils . . . . .	8
2.2.1 Properties of the detection coils . . . . .	9
2.3 Electromagnet . . . . .	11
2.4 Power Supply . . . . .	14
2.5 Sample Theory . . . . .	18
2.5.1 Soft Magnetic Materials . . . . .	21
2.5.2 Magnetic Nanoparticles . . . . .	22
<b>3 Results &amp; Discussion</b>	<b>25</b>
3.1 Electromagnet . . . . .	25
3.2 Power supply . . . . .	27
3.3 Calibration . . . . .	28
3.3.1 Calibration Curve . . . . .	30
<b>4 Conclusions &amp; Outlook</b>	<b>33</b>
<b>A Magnetic Units Conversion</b>	<b>35</b>

<b>B Principal Units of Magnetism</b>	<b>37</b>
<b>Bibliography</b>	<b>39</b>
<b>Abbreviations</b>	<b>43</b>

# List of Figures

2.1	Schematic design of the Faraday Balance Magnetometer . . . . .	4
2.2	Schematic design of the Magneto-Optical Kerr Effect (MOKE) . . . . .	5
2.3	Schematic design of the AC Magnetic Susceptometer . . . . .	6
2.4	Schematic design of the Vibrating Sample Magnetometer (VSM) . . . . .	7
2.5	Permeability for different materials . . . . .	11
2.6	Magnetic field created by a dowel core . . . . .	12
2.7	Magnetic core confines magnetic field . . . . .	13
2.8	Lamination shapes of magnetic cores . . . . .	13
2.9	Magnetic flux density (B) in between the electromagnets poles . . . . .	14
2.10	Full power supply system . . . . .	15
2.11	Transformer image and their symbol . . . . .	16
2.12	Full-wave rectifier . . . . .	16
2.13	Bridge rectifier operation . . . . .	17
2.14	Filter ripple voltage . . . . .	17
2.15	Magnetization curves of ferromagnetic, paramagnetic, superparamagnetic and diamagnetic materials	18
2.16	Saturation curves for different materials . . . . .	19
2.17	Hysteresis loops at different flux densities measured in Tesla units . . . . .	20
2.18	Types of hysteresis loops . . . . .	21
2.19	Hysteresis loop of a soft magnetic material . . . . .	22
2.20	Superparamagnetic behaviour of magnetic nanoparticles . . . . .	23
3.1	Final VSM electromagnet . . . . .	26
3.2	Electromagnet design based on two "E" core shape . . . . .	26
3.3	Transformer, rectifier and capacitor circuit . . . . .	27
3.4	Front panel of the power supply . . . . .	28
3.5	Configuration system disposal . . . . .	28
3.6	Electromagnet poles surface dimension . . . . .	29
3.7	Electromagnet poles distance dimensions . . . . .	29
3.8	Calibration curve . . . . .	30

3.9 Complete system connections . . . . .	31
3.10 Detail of the electromagnet air gap with the Gaussmeter tip inside . . . . .	32

# List of Tables

A.1	Magnetic Units Conversion . . . . .	35
B.1	Principal Units in Magnetism . . . . .	37



# Chapter 1

## Introduction

The spotlight of research up today is based on magnetic nanoparticles which are fascinating nanomaterials with outstanding properties, such as superparamagnetism.<sup>1</sup> Magnetometers belongs to the most common laboratory equipment used to characterize magnetic samples. There exist different types of magnetometers, which are: Superconducting Quantum Interference Device (SQUID), Inductive Pickup Coils, Pulsed-field Extraction Magnetometry, Torque Magnetometry, Faraday Force Magnetometry, Optical Magnetometry, and the Vibrating Sample Magnetometer (VSM).<sup>2</sup>

The VSM is one of the most used equipment, since it can be very sensitive ranging from  $10^{-2}$  to  $10^{-7}$  emu. Additionally, samples can be measured at room temperature or varying the temperature by disposing the appropriate cooling or heating device. VSM is used to measure samples magnetization as function of the applied magnetic external field. This technique represent one of the most important characterization methods in the area of magnetism.<sup>3</sup> Different types of samples can be characterized: macroscopic, microscopic, and nanoscopic.

The area of physics and nanotechnology highly demand characterization methods for magnetic materials (e.g., magnetic nanoparticles). The VSM would provide the characterization method that every undergraduate laboratory requires. The biggest advantage of the VSM is due to its accuracy, versatility and ease of use.<sup>3</sup> The design of the VSM is developed in the next form: 1) electromagnet with its power supply, 2) pick-up coils, 3) audio speaker, 4) lock-in amplifier and signal conditioners, 5) computer interface.

The electromagnet with its power supply provide the necessary magnetic field to drive samples until magnetic saturation. The pick-up coils are used to detect the induced voltage from the magnetized sample. The audio speaker is used to create the oscillatory movement of the sample along the vertical axis on which the sample is perpendicular to the direction of the applied magnetic field. The lock-in amplifier and signal conditioners are used to eliminate the signal noise from the pick-up coils. The computer interface is used to process the signal in order to create the hysteresis loop of the sample.

This thesis work focuses on the first part of the equipment which is the electromagnet with its power supply. This first part is of great importance since the applied field must be high enough to ensure that the sample reaches magnetic saturation. Each magnetic material require different values of applied field to reach magnetic saturation.

The characterization of magnetic samples in an undergraduate laboratory requires a magnetic field of at least 0.5 Tesla.

## 1.1 Problem Statement

The VSM design is set up in the next manner: audio speaker, lock-in amplifier, pick-up coils, computer interface, and electromagnet with its power supply. The challenge lies on the electromagnet magnetic field values which must be higher than 0.2 Tesla in order to magnetize materials. The construction of an electromagnet capable of reaching values up to 0.5 Tesla will contribute for the fabrication of a VSM. This successful achievement will allow students to understand the properties of magnetic materials. Also, the students will improve their knowledge about types of magnetic materials and applications.

## 1.2 General and Specific Objectives

### General Objectives

Construction of an electromagnet and its power supply as the first module of a magnetometer type *Vibrating Sample Magnetometer*.

### Specific Objectives

1. Establish the most suitable materials for the electromagnet core as well as their power supply.
2. Construction of the power supply for the electromagnet.
3. Measurement of the magnetic field in between the electromagnet poles.

## Chapter 2

# Theoretical background

Magnetic Materials are required in a fundamental manner in many fields of science, such as electronic, industry, experimental equipment, devices, etc. This implies that magnetic materials belong to the development of new technology and being crucial their deep studies to know and learn their possible applications. Characterization of magnetic materials starts from the identification of physical and chemical properties which can be used to establish their authentic nature to study their possible applications. The classification of materials based on their magnetic ordering are the next: ferromagnetic, paramagnetic, antiferromagnetic, ferrimagnetic and superparamagnetic, as mentioned in Section 2.5. The main feature about magnetic materials relies on their magnetic moment which is associated to the spin and orbital of electrons. Materials that are exposed to high temperatures, electric current or to an external magnetic field can be magnetized or demagnetized. There exist different techniques to characterize magnetic materials based on their magnetization and magnetic susceptibility that are mentioned next:

**1) Force methods:** This type of technique measures the magnetic susceptibility which is related to the force experienced by the material immersed in a non-uniform magnetic field. This technique has been used in physics laboratories for many years, one of the most common is the Faraday balance which measures the magnetic susceptibility of materials.<sup>4</sup> The basic scheme of the Faraday Balance Magnetometer is shown in Figure 2.1. Another example of force method is the torque magnetometer which consists in applying an external magnetic field in a known direction relative to the sample, and detecting the torque produced. The torque is detected by measuring the restoring torque needed to keep the sample in the original position because the sample is free to rotate and it will try to align to the direction of the applied field.<sup>5</sup>

**2) Magneto-optic methods:** These techniques include measurements of the Faraday effect, analysis of Galvanomagnetic effects, Kerr effect, and microwave ferromagnetic resonance.<sup>4</sup> These techniques are used to calculate magnetization by determining the field strength due to changes of the material optical properties under an applied magnetic field.<sup>7</sup> The most common is the Magneto-Optical Kerr Effect (MOKE) which consists in a laser light source that passes through a polarizer filter to impart a polarization, then the light passes through an objective lens where it is focused onto the sample region of interest. The incident polarized light reflects off the sample surface. There exist different MOKE geometries for the analysis of a sample which are Polar, Longitudinal and Transversal.

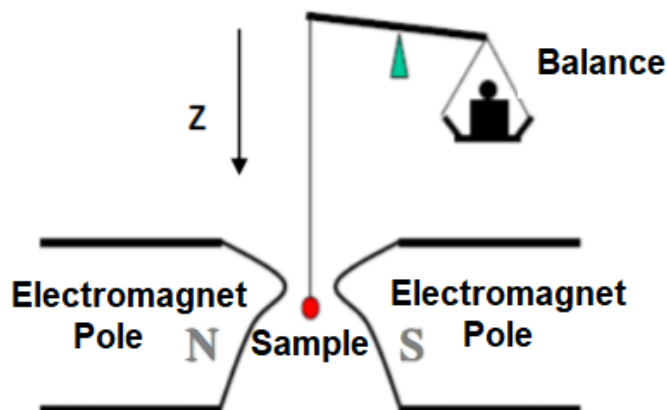


Figure 2.1: The schematic design of the Faraday Balance Magnetometer consists of a sample that is suspended in between poles of magnet in a region of magnetic field gradient. Using a balance, the mass of the sample is registered when the sample is exposed to magnetic field and when it is not. The difference in mass of the sample when it is exposed and when it is not exposed to magnetic field corresponds to the magnetic susceptibility of the sample.<sup>6</sup>

The polarizer have the option to change the polarization of the incident light (circular, linear, and elliptical) based on the MOKE geometries. When the polarized light is reflected off the sample material a change in the following may occur: Kerr rotation, Kerr ellipticity, or polarized amplitude. The changes in polarization are converted by the analyzer into changes in light intensity, which are visible. A computer system is often used to create an image of the magnetic field on the surface from these changes in polarization.<sup>8</sup> See Figure 2.2.

**3) Induction methods:** This type of technique focuses on the measurement of an induced voltage in a detection coil caused by the variation of a magnetic flux; This variation can be generated in different ways, either by varying the applied external field, the position of the search coil, or the position of the sample to be characterized. The ac magnetic susceptometer is an example of induction method where there are three types of coils: excitation coils, pick-up coils and compensation coils. The excitation coils generates an AC magnetic field, the pick-up coils are wound oppositely and the compensation coils eliminate the noise. The voltage measured across the pick-up coils is ideally zero when there is no sample. Inserting a sample centred in one of the pick-up coils will result in a non-zero signal directly proportional to the amplitude of AC.<sup>10</sup> Then, the magnetization and susceptibility of the sample can be measured, see Figure 2.3. Within this type of magnetometers, the most used measurement technique for determining the magnetization of materials is the Vibrating Sample Magnetometer (VSM).<sup>7</sup>

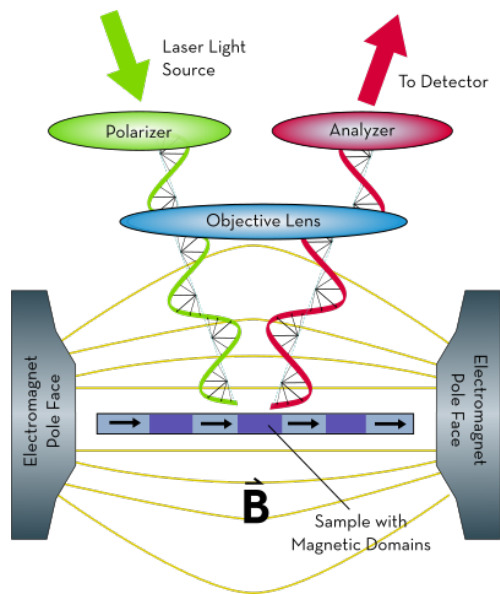


Figure 2.2: The schematic design of longitudinal MOKE consists on a laser light source that passes through a polarizer filter, then the light passes through an objective lens where it is focused onto the sample region of interest. The incident polarized light reflects off the sample surface. The reflected signal passes through an analyzer so that the Kerr rotation signal can be measured. The degree of Kerr rotation can be used to determine the orientation and magnitude of the local magnetic domain because the reflected signal is rotated by the interaction between the polarized probe beam and the magnetic domain structure of the sample.<sup>9</sup>

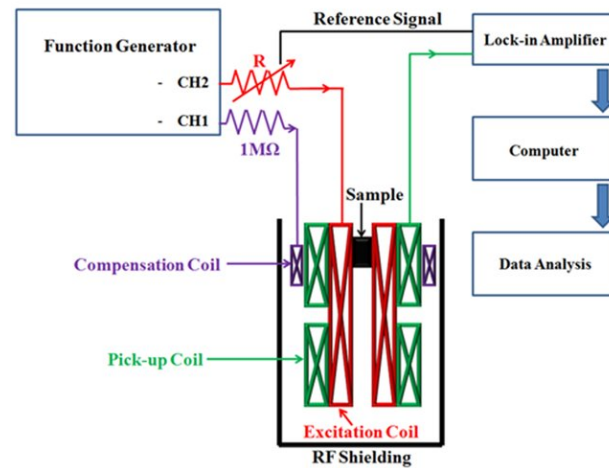


Figure 2.3: The schematic design of the AC Magnetic Susceptometer consists of excitation coils, pick-up coils, and compensation coils. The excitation coils generates an AC magnetic field, the pick-up coils are two coils wound in opposite directions. The compensation coil is used to eliminate or reduce the noise signal. The voltage measured across the pick-up coils is ideally zero when there is no sample. Inserting a sample centred in one of the pick-up coils will result in a non-zero signal directly proportional to the amplitude of AC.<sup>11</sup>

## 2.1 Vibrating Sample Magnetometer

The Vibrating Sample Magnetometer (VSM) was developed by Simon Foner in 1955 and published in 1959. According to Simon Foner<sup>2</sup>, the final purpose of a VSM is to measure the magnetic moment of a sample when it is vibrated perpendicular to a uniform magnetizing field. The VSM has become the "Most used technique" both in basic research laboratories and in production environments, given its ability to measure the basic magnetic properties of materials such as function of external DC magnetic field, temperature and time.<sup>12</sup>

In the studies carried out by Freddy Guachun et al.<sup>4</sup>, it was found that the creation of a VSM with materials from an electromagnetism laboratory stands out compared to other measurement methods due to its simplicity, versatility and low cost. Furthermore, due to its high sensitivity, it is capable of eliminating or minimizing many sources of error found in other measurement methods, thus allowing very precise and reliable results to be obtained. The operation of the VSM is based on the Lenz-Faraday magnetic induction law, which consists of measuring the voltage induced in detection coils produced by the variation of the magnetic flux that passes through them.

The design of a VSM results in placing a vertical vibration head on top of the system, which is connected to a rod that holds the sample at its lower end. This vibration head could be an audio speaker that allows control mechanical vibrations, amplitude, and frequency feedback.<sup>12</sup> An electromagnet is placed to create a horizontal magnetic field in the air-gap where the sample is going to be placed. The detection coils are placed between the electromagnet poles and the sample. The detected signal on the coils is transmitted via a coaxial cable to a blocking electromagnetic noise in the lock-in amplifier. The system is controlled by a selector that allows the variation of the magnetic field

created by the electromagnet, on which a computer interface measures the signal induced in the pickup coils. In this way, the magnetization curves can be recorded at room temperature.<sup>13</sup>

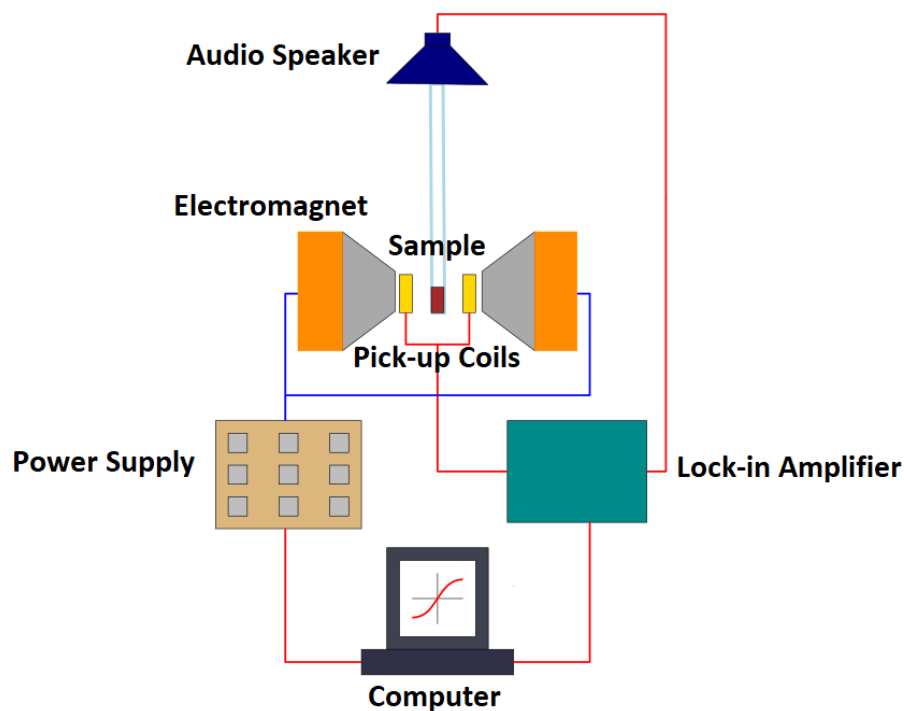


Figure 2.4: Schematic design of the VSM: electromagnet, power supply, audio speaker, sample, pick-up coils, lock-in amplifier and computer.

### 2.1.1 VSM working principle

The VSM working principle starts with the production of magnetic field between the electromagnet poles. The sample is magnetized by the electromagnet's magnetic field due to the aligning of the sample magnetic domains with respect to the applied magnetic field. This means that the sample's magnetic dipole moment creates its own magnetic field sometimes called the magnetic stray field.<sup>14</sup> The up and down motion of the magnetized sample, induces an electric current in the detection coils based on Faraday's Law of Induction. The induced electric current is amplified by a trans-impedance amplifier and lock-in amplifier. Using controlling and monitoring software various components are hooked up to a computer interface. The induced electric current will be proportional to the magnetization of the sample.<sup>14</sup> Finally, the magnetic dipole moment of the sample is tested by measuring the electric current induced in the detection coils. The basic components of the VSM are shown in Figure 2.4 which are the electromagnet with

its power supply, pick-up coils, audio speaker, lock-in amplifier, sample, and computer interface. The electromagnet with its power supply provide the necessary magnetic field to drive samples until magnetic saturation. The power supply can be controlled manually or by a computer interface. The sample can be either a fluid, powder or a solid. The audio speaker is used to create the oscillatory movement of the sample along the vertical axis where the sample is magnetized because is perpendicular to the direction of the applied magnetic field. The pick-up coils are used to detect the induced voltage from the magnetized sample. The lock-in amplifier eliminate the signal noise from the pick-up coils. The computer interface processes the signal in order to create the hysteresis loop of the sample.

## 2.2 Detection Coils

The VSM have 3 different known configurations for detection coils named as: 1) Foner, 2) Mallison, and 3) Bowden. The Foner configuration is based on two pick-up coils connected in series to obtain a net output signal. This configuration eliminates the background noise caused by the instability of the magnetic field or mechanical vibrations of the electromagnet and coil systems.<sup>2</sup> The Mallison configuration have four pick-up coils in series with their axes parallel to the x-axis. This configuration has a maximum signal when the coils are join together at an angle of 45° on the sides of the sample.<sup>4</sup> The Bowden configuration consists of eighth pick-up coils in series with their axes parallel to the y-axis. This configuration showed stability for the saddle points at the sample space.<sup>15</sup>

The pick-up coils are assembled either parallel or perpendicular to the direction of the magnetic field generated from the electromagnet poles. The vertical movement of the magnetized sample produces a change in the magnetic flux that induces a voltage  $V_{ind}$  in the detection coils.<sup>16</sup> According to Faraday's Law of Induction, the voltage in a single winding of the pick-up coil can be written as:

$$V_{ind} = -\frac{d\Phi}{dt}, \quad (2.1)$$

where the magnetic flux is  $\Phi$ . Let's consider a flat surface  $A$  with the number of pick-up coils  $n_c$  and its windings  $n_w$ , equation 2.1 become:

$$V_{ind} = \sum_{n_c} \sum_{n_w} \int_A \frac{\partial \vec{B}}{\partial t} \cdot d\vec{A}. \quad (2.2)$$

As the sample is magnetized along the x-axis by the electromagnet magnetic field, a resulting sample magnetic moment  $\vec{m}$  is produced. The sinusoidal movement  $\vec{\delta}(t)$  of the sample along the z-axis is described in the next equation, being  $Z$  the amplitude,  $\omega$  the frequency:

$$\vec{\delta}(t) = \frac{dz}{dt} = Z\omega \cos(\omega t). \quad (2.3)$$

The change in the magnetic flux density  $\vec{B}$ , its due to the sample's magnetic moment. Then, for a point at a distance  $\vec{r}$  from the sample, being  $\mu_0$  the magnetic permeability of free space,  $\vec{H}$  the field strength:

$$\frac{\partial \vec{B}(t)}{\partial t} = \mu_0 \cdot \vec{\delta}(t) \cdot \vec{\nabla}\{\vec{H}(\vec{r})\}, \quad (2.4)$$

$$\vec{H}(\vec{r}) = \frac{1}{4\pi} \left( \frac{\vec{m}}{r^3} - \frac{3(\vec{m} \cdot \vec{r})\vec{r}}{r^5} \right). \quad (2.5)$$

Finally, the change of magnetic flux detected by the coils is proportional to the frequency  $\omega$  of the sample's vibration, with its amplitude  $A$ , and the sample's magnetic moment  $\vec{m}$ . Moreover, the addition of number of windings  $n_w$  and the number of pick-up coils  $n_c$  will increase the induced voltage  $V_{ind}$ .

### 2.2.1 Properties of the detection coils

The pick-up coils are organized with axes parallel or perpendicular to the field direction as well as the direction of vibration-axis of the sample with respect to magnetizing field direction.<sup>17</sup> The superconducting magnet is an example on how the solenoidal magnetic fields require that the axes of the detection coils and sample vibration must be parallel to the magnetic moment. After all, this geometry of detection coils is inconvenient for conventional iron-core electromagnets as it requires special modifications to the poles faces.<sup>17</sup> Some of the main features that detection coils must follow in order to determine a proper arrangement:

- To minimize effect of noise from external magnetic disturbance, there must be a proper compensation of pick-up coils.
- It is required to have a broad saddle point whereby the signal is immune to small changes in the main position of the sample.
- Maximization of signal-to-noise (Johnson noise) ratio by optimizing the dipole flux linkage with coils.
- Enough space for a cryostat tail in the the air-gap between the electromagnet poles.
- Ease of sample change and alignment of the sample-rod.

The improvement of the induced voltage is based on Faraday's Law of Induction which stands that:

"Any change in the magnetic environment of a coil of wire will cause a voltage to be induced in the coil. No matter how the change is produced, the voltage will be generated. The change could be produced by changing the magnetic field strength, moving a magnet toward or away from the coil, moving the coil into or out of the magnetic field, rotating the coil relative to the magnet, etc."<sup>18</sup>

Faraday's experiments showed that a change in magnetic flux induces an Electromotive force (EMF) that depends on only a few factors. First, the change in flux  $\Delta\Phi$  is directly proportional to the EMF. Second, EMF is inversely proportional to  $\Delta t$  because EMF is bigger when the change in time  $\Delta t$  is smaller. Finally, if a coil has  $N$  turns, an EMF will be  $N$  times greater than for a single coil, so that EMF is directly proportional to  $N$ . The equation for the EMF induced by a change in magnetic flux is:

$$\text{EMF} = -N \frac{\Delta\Phi}{\Delta t}. \quad (2.6)$$

Faraday's Law of Induction states that a changing magnetic field produces an electric field where EMF is the electromotive force,  $\Phi$  is magnetic flux.

Lenz's Law describe that an EMF creates a current  $\vec{I}$  and magnetic field  $\vec{B}$  that opposes the change in flux  $\Delta\Phi$ . Lenz' law explains a manifestation of the conservation of energy. The induced EMF produces a current that opposes the change of magnetic flux, because a change in magnetic flux means a change in energy. Energy can enter or leave, but not instantaneously.<sup>19</sup> Then, when the sample dipole moment moves along the z-axis with a motion  $z(t) = Z\sin(\omega t)$ , the net axial component of  $\vec{B}(\vec{r})$  through coil 1 increases in the downward direction, while in coil 2 increases in the upward direction. Since the coil turns are in the same direction, the combined EMF of the two coils add up at the terminal to give a net signal free of external noise.<sup>17</sup>

Based on Faraday's Law of Induction and Lenz's Law, the increase of the EMF on the pick-up coils could be achieved by increasing the surface  $S$  of the sample and using ferromagnetic core with a high number of windings  $N$  in the coil.

The improvement of the pick-up coils would optimize the detection of the change in the magnetic flux produced by the magnetized sample. The magnetic flux common denoted as " $\Phi$ " or " $\Phi_B$ " is the component of the magnetic field passing through a surface. The magnetic flux through some surface is proportional to the number of field lines passing through that surface. In this case, the surface would be the sample surface area. The magnetic flux is represented in the next equation:

$$\Phi = \vec{B} \cdot \vec{A} = BA \cos\theta, \quad (2.7)$$

where  $\vec{B}$  is the magnitude of the magnetic field (having the unit of Tesla, "T"),  $A$  is the area of the surface, and  $\theta$  is the angle between the magnetic field lines and the normal (perpendicular) to  $A$ . For a varying magnetic field, we first consider the magnetic flux  $d\Phi$  through an infinitesimal area element  $d\vec{A}$ , where we may consider the field to be constant:

$$d\Phi = \vec{B} \cdot d\vec{A}. \quad (2.8)$$

The surface " $A$ ", can then be broken into infinitesimal elements and the total magnetic flux through the surface is then the surface integral:

$$\Phi = \iint_A \vec{B} \cdot d\vec{A}. \quad (2.9)$$

The same principal happens for a loop of wire expose to a magnetic field that depends on time where the magnetic flux  $\Phi$  is defined for any surface  $A$  whose boundary is the given loop. Since the wire loop might be moving,  $A$  is denoted as the surface.

## 2.3 Electromagnet

The fabrication of an electromagnet is essentially based on the magnetic flux created when a current passes through a coiled wire.<sup>20</sup> The explanation of this phenomena is referred as electromagnetism, which is a branch of physics that studies the relation between magnetism and electricity. The basic definition of electromagnetism establish that a magnetic field is created along a conductor material, such as a copper wire, when an electrical current flows along the whole conductor material. The magnetic field created around the conductor material has a defined direction, which is referred as the north pole and south pole, resulting from the direction of the electrical current flow that goes through.<sup>21</sup> The magnetic field generated by an electric current can be calculated by the Biot-Savart Law.<sup>22</sup>

$$d\vec{B} = \frac{\mu_0}{4\pi} \frac{I d\vec{\ell} \times \hat{r}}{r^2}, \quad (2.10)$$

where  $\mu_0$  is the permeability of free space, the  $d\vec{\ell}$  is the length contribution of an infinitesimal element, the current  $I$  that passes through a coiled wire, and generates a magnetic field  $d\vec{B}$ , perpendicular to the plane formed by the vector  $d\vec{\ell}$  and  $\hat{r}$ , at a distance  $r$  with respect to  $d\vec{\ell}$ , that points in the direction of current  $I$ . The Equation 2.10, enable to calculate the magnetic field  $\vec{B}$  generated by an electrical current passing through an elementary length of a conductor. This fundamental law is a statement of experimental observation rather than a theoretical prediction. The magnetic field decreases with square of the distance from the current element that produces it.<sup>22</sup> Then, the generation of magnetic field would be determined due to basic parameters which are the permeability of the magnetic core, length of the coil, and amount of current passing through the coil.

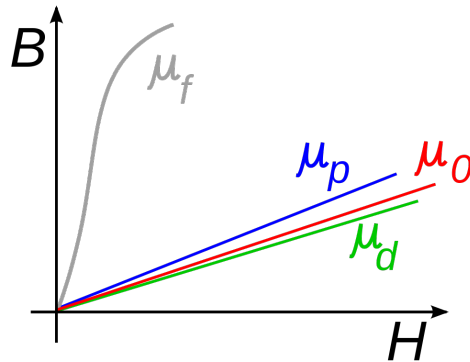


Figure 2.5: Simplified comparison of permeabilities for: ferromagnets ( $\mu_f$ ), paramagnets ( $\mu_p$ ), free space ( $\mu_0$ ) and diamagnets ( $\mu_d$ ).<sup>23</sup>

The capacity of a material to conduct magnetic flux is defined as permeability.<sup>20</sup> In essence, the magnetic permeability " $\mu$ " measures the material's strength to support on how much magnetic flux passes through it. In Figure 2.5, the magnetic field strength  $\vec{H}$  represents how a magnetic induction or flux density  $\vec{B}$  influences the organization of magnetic dipoles in a given material, including dipole migration and magnetic dipole reorientation. Ferromagnetic

materials, such as, iron, nickel, cobalt and their alloys exhibit high values of permeability compared to paramagnetic and diamagnetic materials, as shown in Figure 2.5. Magnetic permeability can also be refer to be the materials magnetization capability.<sup>24</sup> The ratio between the flux density  $\vec{B}$ , and the field strength  $\vec{H}$  is defined as permeability  $\mu$ .<sup>25</sup>

$$\vec{H}\mu = \vec{B}. \quad (2.11)$$

Another important concept to emphasize is the relative permeability, denoted by the symbol  $\mu_r$ , which is the ratio of the permeability of a specific medium to the permeability of free space  $\mu_0$ :

$$\mu_r = \frac{\mu}{\mu_0}, \quad (2.12)$$

where  $\mu_0 \approx 4\pi \times 10^{-7} \text{N} \cdot \text{A}^{-2}$  is the magnetic permeability of free space. In terms of relative permeability, the magnetic susceptibility is:

$$\chi_m = \mu_r - 1. \quad (2.13)$$

The number  $\chi_m$  is a dimensionless quantity, sometimes called volumetric or bulk susceptibility, to distinguish it from  $\chi_p$  (magnetic mass or specific susceptibility) and  $\chi_M$  (molar or molar mass susceptibility).

In Figure 2.6, current  $I$  pass through a coil wire on a dowel creating a magnetic flux  $\Phi$ . In this case a dowel is used as a core material. Then, magnetic field can be produced even by a wire wound on a dowel, as shown in Figure 2.6, but only materials that have high values of permeability are used as based for core materials. These core materials have an important role that is to contain the magnetic flux and create a well-defined predictable path for the flux.<sup>20</sup> The flux path and the mean distance covered by the flux within the magnetic material, is defined as Magnetic Path Length.<sup>20</sup>

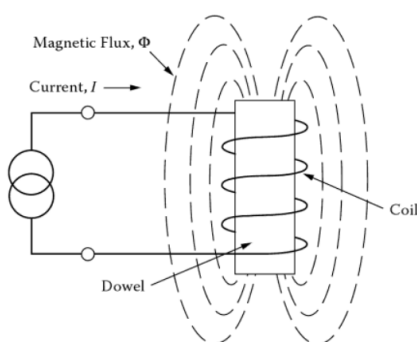


Figure 2.6: Magnetic flux  $\Phi$  is created by current  $I$  that pass through a coil wire on a dowel.<sup>20</sup>

In Figure 2.7, the magnetic core contain the flux where the magnetic path length is showed as the mean distance covered by the flux. The permeability and the magnetic path length are important parameters in prediction the characteristic operation of the magnetic device. The selection of a core material will strictly depend on the size, weight, temperature rise, flux density, core loss, and operating frequency.

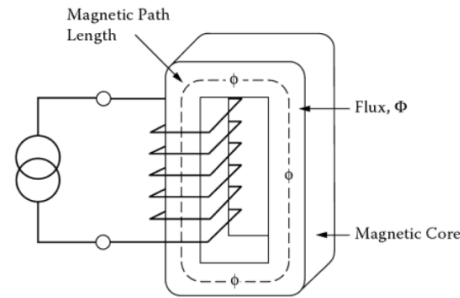


Figure 2.7: Magnetic core confines the magnetic flux where the Magnetic Path length is described as the mean distance covered by the flux.<sup>20</sup>

There exist two types of magnetic cores which are the shell type and the core type. In the shell type, the core surrounds the coil and the magnetic field is around the outside of the coil. In the core type, the coils are outside of the core which a good example is a "Toroid" where the coil is wound outside of the core.<sup>20</sup> There is another important parameter for the construction of magnetic devices, called Lamination. In Figure 2.8, it is shown that there exist different shapes of laminations which are EI, EE, FF, UI, LL, and the DU. Each lamination shape differs from each other by the location of the cut in the Magnetic Path Length. The cut introduces an air gap, which results in the loss of permeability. When laminations are stacked, there is a flux crowding. The difference in spacing between the E, I and adjacent lamination causes flux crowding which results in higher permeability.<sup>20</sup> Magnetic cores are made of iron laminate which are separated by a thin layer of an insulator that most cases is varnish. This structure of iron laminate and insulator reduces eddy currents.<sup>26</sup>

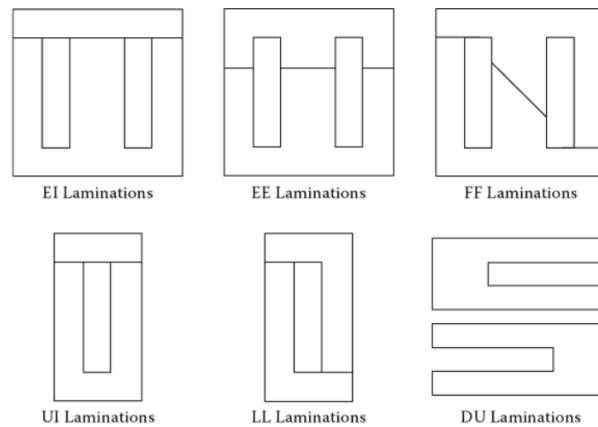


Figure 2.8: Lamination shapes are divided into: EI, EE, FF, UI, LL, and DU. Each lamination differs from each other by the location of the cut in the Magnetic Path Length.<sup>20</sup>

The surface area of the electromagnets poles from which the magnetic flux density come out is an important parameter for the develop of the VSM. The basic concept of magnetic flux density  $\vec{B}$  is define as the number of magnetic flux lines per unit area passing through a plane perpendicular to the direction of the lines. Electromagnets have poles which can be referred as north pole and south pole. In Figure 2.9, the magnetic flux density goes from the north pole to the south pole. Electromagnets generate magnetic flux which can be described by Equation 2.7. As the surface area of the electromagnet pole decreases, the magnetic flux density  $\vec{B}$  increases because they are inversely proportional.

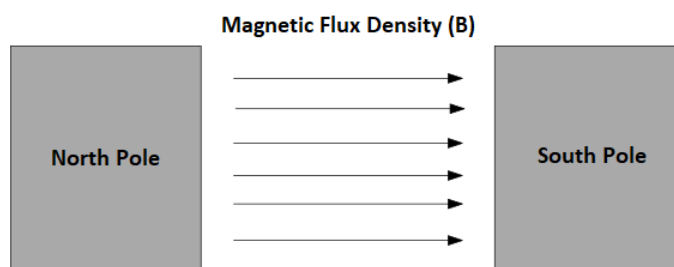


Figure 2.9: Magnetic flux density (B) in between the electromagnets poles.

The unit used for measuring magnetic flux lines is Weber (Wb) and the unit for measuring magnetic flux density is Tesla (T), See Equation 2.14. Finally, the surface area of the electromagnets poles should be reduced in order to achieve high values of magnetic field. See Figure 2.9

$$1 \text{ Tesla} = \frac{1 \text{ Weber}}{1 \text{ m}^2}. \quad (2.14)$$

## 2.4 Power Supply

Electronic devices, in order to work, require a source of constant DC such as a battery or a DC power supply. The operation of the VSM's electromagnet, highly requires a DC power supply. The traditional DC power supply converts 120 v, 60Hz AC voltage in constant DC voltage. The basic diagram of a complete power supply is shown in Figure 2.10. The main parts are the transformer, rectifier, filter, regulator and load.

The type of transformer used in this thesis is a voltage step-down transformer. The current at the primary coil produces a magnetic field almost totally contained in the iron core and couples around through the secondary coil. The iron core in the primary coil, trap the magnetic field and increase the field strength. Since the input voltage is AC, a time-varying magnetic flux is sent to the secondary, inducing its AC output voltage.<sup>19</sup> The induced voltage in the secondary voltage is given by  $V_s = -N_s A \frac{\Delta \vec{B}}{\Delta t}$ . Transformers cannot increase power so that if the voltage is

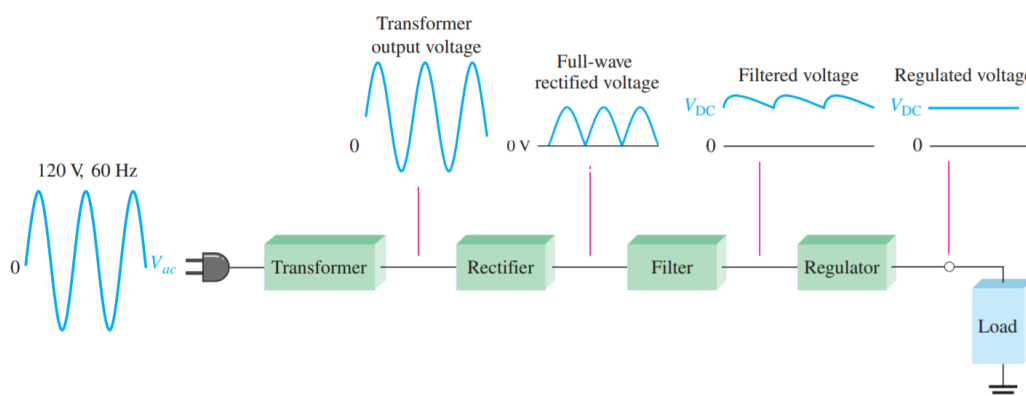


Figure 2.10: The full power supply system consists of a transformer to stepped down the ac input line voltage to a lower ac voltage. Then, a rectifier is used to convert the ac input voltage to a pulsating dc voltage, called a full-wave rectified voltage. Then, a filter is used to eliminate the fluctuations in the rectified voltage and to produce a relatively smooth dc voltage. Finally, a regulator is used to maintain a constant dc voltage.

raised, the current is proportionally lowered and vice versa. Most common transformers are made of ferromagnetic materials, such as, the iron core which efficiently raise or lower AC voltages.<sup>27</sup>

$$\frac{V_S}{V_P} = \frac{N_S}{N_P}, \quad (2.15)$$

the voltage ratio (" $V_S$ " the voltage at the secondary coil, " $V_P$ " the voltage at the primary coil) is equal to the turns ratio (" $N_S$ " the turns of the secondary coil, " $N_P$ " the turns for the primary coil).

$$P_P = V_P I_P = V_S I_S = P_S, \quad (2.16)$$

also the power-in equals power-out based on the energy conservation law. Hence, " $P_P$ " power at the primary coil equals " $P_S$ " power at the secondary coil.

Based on equation 2.15, if the secondary coil has more turns than the primary, then the output voltage across the secondary will be higher and the current will be smaller. Now, if the secondary coil has fewer turns than the primary, then the output voltage across the secondary will be lower and the current will be higher.

In Figure 2.11 there is an example of a simple transformer with two coils wound on either sides of a laminated ferromagnetic core. The set of coil on left side of the core is marked as the primary and there number is given as  $N_P$ . The voltage across the primary is given by  $V_P$ . The set of coil on right side of the core is marked as the secondary and the number of turns is represented as  $N_S$ . The voltage across the secondary is given by  $V_S$ . A symbol of the transformer is also shown below the diagram. It consists of two inductor coils separated by two equal parallel lines representing the core.<sup>19</sup>

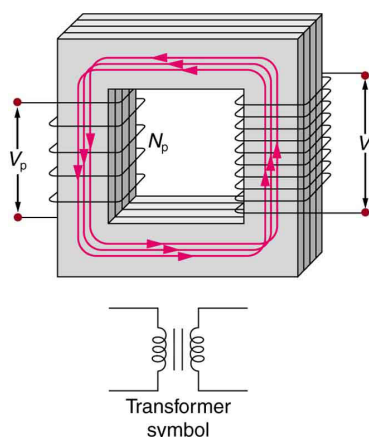


Figure 2.11: A typical construction of a simple transformer has two coils wound on a ferromagnetic core that is laminated to minimize eddy currents. The magnetic field created by the primary is mostly confined to and increased by the core, which transmits it to the secondary coil. Any change in current in the primary induces a current in the secondary.<sup>19</sup>

The rectifier converts the AC input voltage to a pulsating DC voltage, called a full-wave rectified voltage, as shown in Figure 2.12. The full-wave rectifier allows unidirectional (one-way) current through the load during the entire  $360^\circ$  of the input cycle.

The full-wave bridge rectifier is going to be used for the circuit of the VSM power supply. This bridge rectifier uses four diodes connected as shown in Figure 2.13. There exist the positive half-cycle and negative half-cycle. During the positive half-cycle of the input as shown in part (a) Figure 2.13, diodes  $D_1$  and  $D_2$  are forward-biased and conduct current in the direction shown. Across  $R_L$  a voltage is developed from the positive half of the input cycle and at the same time, diodes  $D_3$  and  $D_4$  are reversed-biased. During the negative half-cycle of the input as shown in part (b) Figure 2.13, diodes  $D_3$  and  $D_4$  are forward-biased and conduct current in the same direction through the equivalent resistance load ( $R_L$ ) as during the positive half-cycle, and at the same time  $D_1$  and  $D_2$  are reversed-biased. Finally, a full-wave rectified output voltage appears across  $R_L$  as a result of this process.<sup>28</sup>

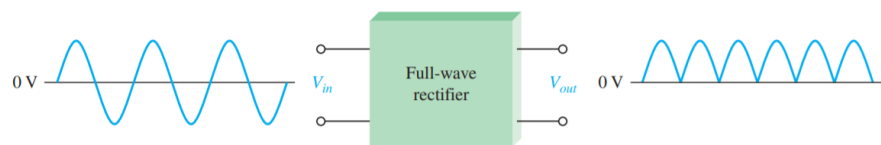


Figure 2.12: Full-wave rectifier converts the AC input voltage to a pulsating DC voltage.<sup>28</sup>

The power supply of this thesis project uses a full-wave bridge rectifier with a transformer-coupled input which provides two advantages. First, the transformer-coupling allow the source voltage to be stepped down as needed.

Second, the AC source is electrically isolated from the rectifier, thus preventing a shock hazard.

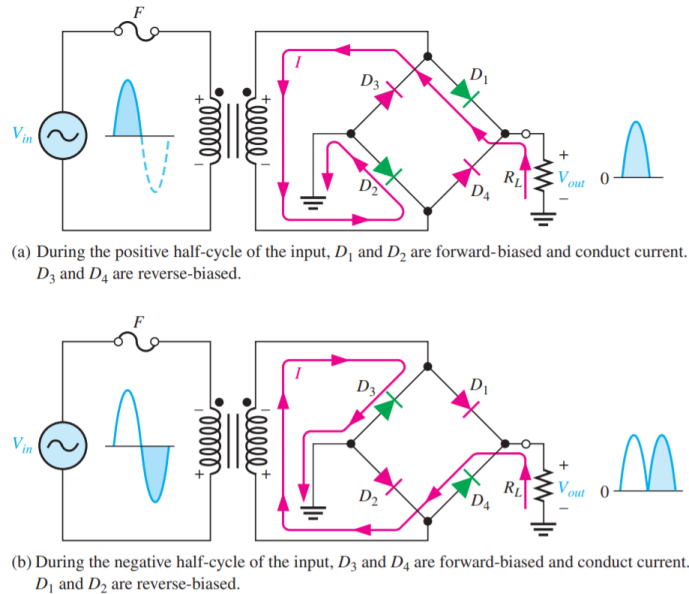


Figure 2.13: Bridge Rectifier Operations consist of two cycles which are the positive half-cycle and negative half-cycle. a) Positive half-cycle of the input:  $D_1$  and  $D_2$  are forward-biased and conduct current, while  $D_3$  and  $D_4$  are reversed-biased. b) Negative half-cycle of input:  $D_3$  and  $D_4$  are forward-biased and conduct current, while  $D_1$  and  $D_2$  are reversed-biased.<sup>28</sup>

The next component of the power supply is the filter which eliminates the fluctuations in the rectified voltage and produces a smooth DC voltage as shown in Figure 2.10. The full-wave rectifier must be filtered to reduce the large voltage variations.<sup>28</sup>

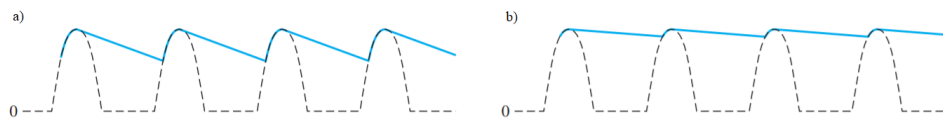


Figure 2.14: a) Larger ripple voltage which means less effective filtering. b) Smaller ripple voltage which means more effective filtering. Generally, the larger capacitor value, the smaller the ripple for the same input and load.

The filter consist of a capacitor connected from the rectifier output to ground. The capacitor quickly charges at the beginning of a cycle where the diode is forward-biased and happens only once when power is turned on. Then, the capacitor slowly discharges through  $R_L$  after the positive peak alternation when the diode is reversed-biased.<sup>28</sup> Finally, the capacitor charges back to peak of input when the diode becomes forward-biased. The variation in the

capacitor voltage due to the charging and discharging is called the ripple voltage.<sup>28</sup> The smaller the ripple, the better the filtering action as shown in Figure 2.14.

The final component is the voltage regulator which is connected to the output of a filtered rectifier and keep a constant output voltage or current, despite changes in the input, the load current or the temperature.<sup>28</sup> The capacitor-input filter reduces the input ripple to the regulator. The best power supply is a combination of a large capacitor-input filter and a voltage regulator. The most common regulators are integrated circuits that have three terminals, the input terminal, output terminal, and a reference terminal.<sup>28</sup> The input terminal is connected to the capacitor-input filter that reduce the ripple around 10%. The regulator has the ability to reduce the ripple to a negligible amount. Additionally, regulators have an internal voltage reference, short circuit protection, and thermal shutdown circuitry.

In order to fabricate an electromagnet for a VSM, it is fundamental to have a high magnetic field provided from the electromagnet. The most suitable way to achieve high values of magnetic field is connecting transformers in series. Based on Faraday's law of induction (equation 2.6) and Biot-Savart law (equation 2.10), the increase of current is proportional to the magnetic field generated from the electromagnet. This approach will allow to increase the magnetic field of the electromagnet due to the current from the connection of transformers in series. The complete power supply for this thesis project would be the nine transformers connected in series, the full-wave bridge rectifier diode, capacitor-input filter, and a regulator.

## 2.5 Sample Theory

Materials exhibit different properties according to their magnetic response to an applied magnetic field. All materials experience magnetism, is just that some materials more than others. The quantum mechanics of atoms and molecules describe the basis of magnetism according to the magnetic moment associated to the orbital and spin of electrons.

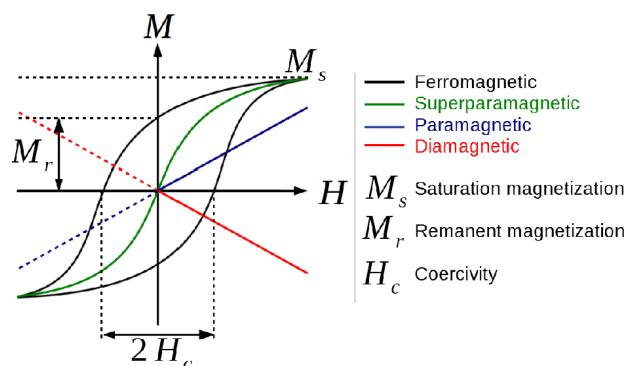


Figure 2.15: A typical magnetization graph of ferromagnetic, paramagnetic, superparamagnetic and diamagnetic materials.<sup>29</sup>

Materials can be classified according to their magnetic response to an applied magnetic field. Paramagnetism exhibit materials that are weakly attracted by an applied magnetic field on which the material creates its own magnetic

field in the same direction of the applied magnetic field. This happens due to the presence of unpaired electrons in the material or to the partial alignment of randomly oriented atomic dipoles along the field.<sup>30</sup> This type of material do not retain magnetization when the external applied magnetic field is removed as shown in Figure 2.15.

Diamagnetism is display in materials that are repelled by magnetic fields. This happens because a repulsive force is originated due to the creation of the material's own magnetic field in the opposite direction of the applied magnetic field.

Antiferromagnetism happens at low temperature and could be disrupted by heating and disappear entirely above a certain temperature, called the Néel temperature.<sup>31</sup> This type of materials align antiparallel their atomic dipoles when there is an applied magnetic field, which results in a low magnetization.

Ferrimagnetic materials are described by the alignment of atomic dipoles in the same direction (like ferromagnetism) to the applied field and other atomic dipoles from sublattices pointing in the opposite direction that have a small contribution.<sup>32</sup>

Ferromagnetic materials exhibit an exclusive phenomenon where they are magnetized when an external magnetic field is applied. The atomic dipoles in small regions which are called domains, aligned in the same direction and exhibit a net magnetic moment even in the absence of the external magnetic field. Before magnetization, the material presents a random domain orientation where the net magnetic moment is zero due to the cancel out of each domain's magnetic moment. After magnetization, which is the applied of an external magnetic field to the material; the domains align in the direction of the applied magnetic field.<sup>33</sup>

Superparamagnetism is a new form of magnetism which is based on magnetic nanoparticles that can randomly flip their magnetization under the influence of temperature.<sup>34</sup> These magnetic nanoparticles are considered as a single magnetic domain due to the sum of all individual magnetic moments from the nanoparticles that contribute to the net magnetization. The remanent magnetization and coercivity from the magnetic nanoparticles are both zero.

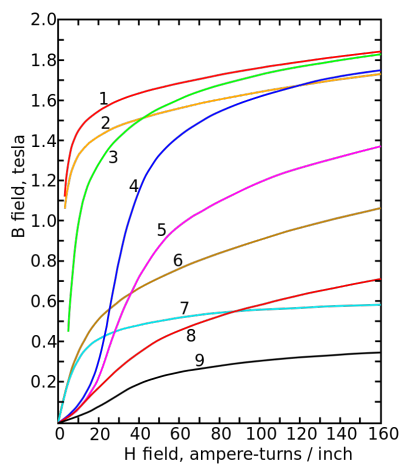


Figure 2.16: Magnetization curves of 9 ferromagnetic materials, showing saturation. 1. Sheet steel, 2. Silicon steel, 3. Cast steel, 4. Tungsten steel, 5. Magnet steel, 6. Cast iron, 7. Nickel, 8. Cobalt, 9. Magnetite.<sup>35</sup>

The VSM is used to characterize different materials by studying their magnetization under an applied magnetic field, as shown in Figure 2.15. The most important parameter is the magnetic saturation which is the value that indicates if material is completely magnetized. Magnetization curves of different materials are shown in Figure 2.16.

However, the VSM yield a hysteresis loop from which magnetic materials can be characterized. The study of magnetic materials begins with the "history dependent" nature display in the hysteresis loop.

The applied magnetic field  $\vec{H}$  in Ampere per meter [A/m] or Oersted [Oe] units which is the strength need it to create flux lines; is represented in the x-axis. The flux density in Tesla [T] units, which is the number of flux lines that have been created; is represented in the y-axis.

The magnetizing curve is the increase of flux lines  $\vec{B}$  due to the increase of magnetizing strength  $\vec{H}$ . The magnetizing curve will get a saturation level where no matter how much magnetizing strength is increase, there are no more flux lines created. The result is the magnetic saturation of the material. Different materials exhibit different saturation levels. For example, high permeability iron alloys used in transformers reach magnetic saturation at 1.6–2.2 T, whereas ferrites saturate at 0.2–0.5 T. Some amorphous alloys saturate at 1.2–1.3 T.<sup>36</sup> Mu-metal saturates at around 0.8 T.<sup>37</sup> Magnetic nanoparticles saturates around 0.1-0.2 T.<sup>38</sup>

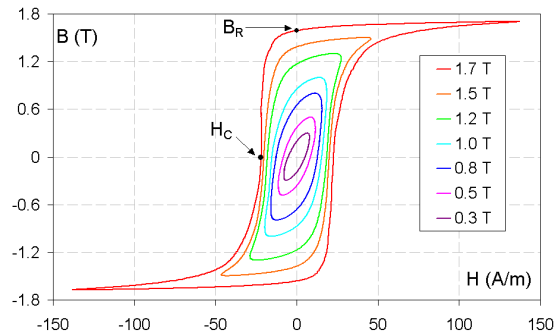


Figure 2.17: A family of B-H loops measured with a flux density that is sinusoidally modulated at 50 Hz with amplitude varying from 0.3 T to 1.7 T. The material is conventional grain-oriented electrical steel.  $B_r$  denotes the remanence and  $H_c$  is the coercive field. The B-H loop is another name for hysteresis loop.<sup>39</sup>

After the material is magnetized until saturation, the magnetization strength  $H$  is give away until zero. Then, the material retain some flux lines, which is call remanent magnetization, retentive or retention which is denoted as  $B_r$ . In order to get rid of the retention magnetism, there must be a magnetization strength in the opposite direction. Then, the flux lines are drop down to zero. The field strength use to drop the flux lines to zero is called coercive field or coercivity  $H_c$ .

If the magnetic strength keep increasing in the opposite direction, a magnetization curve will be created in the same direction as the flux lines increase until a saturation point. After the material is magnetically saturated, the magnetic strength  $H$  is turned off and there is a drop of flux lines where the material will remanent magnetism  $B_r$ . Again, the magnetic strength  $H$  is increase in the positive direction where the coercivity  $H_c$  appears and the flux lines goes to zero. Finally, the magnetic strength  $H$  is turn on until saturation to complete the hysteresis loop or B-H

loops, see Figure 2.17.

The hysteresis could provide information about the magnetization's material. Skinny hysteresis could mean that the material do not retain magnetism and also it would need very little energy to overcome the barrier to switch the direction of magnetic moment when magnetization switches. This type of materials could be useful for the creation of transformers, electromagnets, and motors. This materials are named as soft materials which have very low magnetic retention.

For fat hysteresis, the material is known to retain magnetism which means that the material will require more energy to overcome the barrier in order to switch the direction of magnetic moment when magnetic field switches. An interesting application could be for memory storage, in which the material must retain magnetism in order to not switch easily their magnetic moments due to the high energy barrier that is not easy overcome when switching magnetic field.

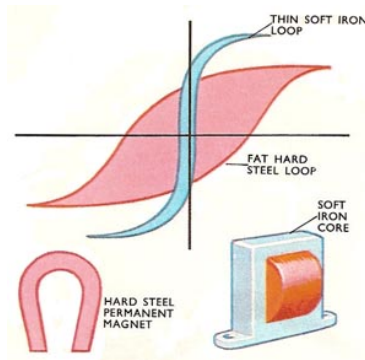


Figure 2.18: This image shows the different types of hysteresis. Fat hysteresis represent hard steel permanent magnets. For thin hysteresis, it represents soft iron cores.<sup>40</sup>

### 2.5.1 Soft Magnetic Materials

In this thesis project, the soft magnetic materials are the target to be characterize by the VSM. Materials that are easily magnetized and demagnetized are called soft magnetic materials. The main parameter is the relative permeability  $\mu$  which is a measure of how a material responds to an applied magnetic field. The other parameters are the saturation magnetization and the electrical conductivity.<sup>41</sup>

Soft materials are use for DC and AC applications. For DC applications, the material is magnetized in order to perform an operation and then demagnetized at the end of the operation. An electromagnet is a good example. In the case of an electromagnet on a crane at a scrap yard will be switched on to attract the scrap steel and then switched off to drop the steel. The main consideration to select a material, is the permeability. For example, in shielding applications where the flux must be channelled through the material. In addition, the saturation magnetisation is very significant parameter when the material is going to be use to generate a magnetic field.<sup>41</sup>

For AC applications, the material is continuously cycled from being magnetized in one direction to the other, throughout the period of operation. For example, a power supply transformer. A high permeability is desired for each type of application but the virtue of the other properties varies.

A highly important parameter is how much energy is lost in the system as the material is cycled around its hysteresis loop. The energy loss can originate from three different sources: hysteresis loss, the eddy current loss, and anomalous loss.

The hysteresis loss is related to the area contained within the hysteresis loop as shown in Figure 2.19. The eddy current loss occurs when electrical currents are induced inside the material by the flux lines passing through it. The anomalous loss is related to the movement of magnetic domain walls within the material.<sup>41</sup>

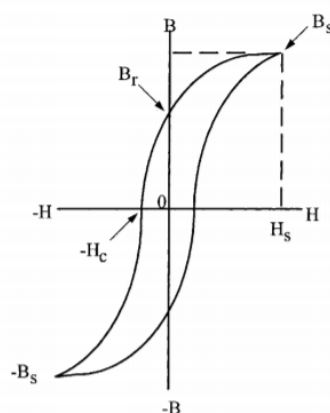


Figure 2.19: B-H loop of a soft magnetic material where  $B_s$  is magnetic flux saturation,  $H_s$  is field strength saturation,  $B_r$  is remanent magnetization, and  $H_c$  is the coercive field.<sup>25</sup>

## 2.5.2 Magnetic Nanoparticles

Magnetic Nanoparticles (MNPs) can appear inside the classification of soft magnetic materials. Their applications are numerous in the field of Nanotechnology, Biotechnology, and Nanomedicine. The principal properties of magnetic nanoparticles start with their size which can be compared to a virus (20-500 nm), protein (5-50 nm), or a gene (2 nm wide and 10-100 nm long).<sup>1</sup> The magnetic nanoparticles have an interesting advantage which is a large surface area that can be properly modified to attach biological agents. In addition, the magnetic nanoparticles can be manipulated by an external magnetic field gradient.<sup>1</sup>

Iron oxide magnetic nanoparticles ( $\text{Fe}_3\text{O}_4$  and  $\text{Fe}_2\text{O}_3$ ) have outstanding properties, such as easy preparation, low cost, simple surface functionalization, and biocompatibility. These properties make Fe oxide materials ideal candidates for designing nanohybrid platforms for drug delivery.<sup>42</sup> The principal advantage of the iron oxide nanoparticles is their superparamagnetic behaviour which is ideal for drug delivery and targeting. Superparamagnetism allows

delivering the drug-loaded nanohybrid system to the tumor site under the influence of an external magnetic field, and after the external magnetic field is removed, the material loses its magnetization.<sup>42</sup>

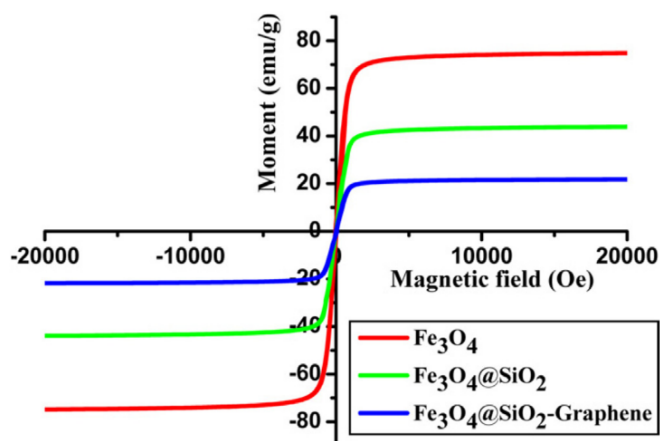


Figure 2.20: Superparamagnetic behaviour of magnetic nanoparticles: Fe<sub>3</sub>O<sub>4</sub> MNPs (red), Fe<sub>3</sub>O<sub>4</sub> MNPs coated with SiO<sub>2</sub> (green), Fe<sub>3</sub>O<sub>4</sub> MNPs coated with SiO<sub>2</sub>/Graphene (blue).<sup>38</sup>

The VSM can evaluate the property of superparamagnetism in the iron oxide nanoparticles which require no more than 0.5 Tesla of applied magnetic field to get until saturation. An example of magnetization curves of magnetic nanoparticles are described in Figure 2.20. Another interesting application of MNPs is for tumor cells treatment which is named as Hyperthermia. This novel treatment requires MNPs that when they are placed in an alternating magnetic field of high frequency, they can produce sufficient heat due to the hysteresis loop of the magnetic material and induce eddy currents when a variable external magnetic field is applied.<sup>1</sup> The VSM plays an important role for the generation and analysis of hysteresis loop. The electromagnet with its power supply are crucial to produce magnetic saturation on MNPs. The use of a VSM would provide important results for MNPs applications.



## Chapter 3

# Results & Discussion

Vibrating sample magnetometers require high values of magnetic field in order to achieve saturation and the study of materials' remanence and coercivity. The electromagnet with its power supply are a fundamental part for the generation of a high magnetic field. As mentioned in Chapter 2 section 2.5, the remanence is the polarized flux remaining in the material after the field strength has been removed. The coercivity is the amount of magnetizing force or field strength required to bring the remanence density back to zero. Soft materials are easily magnetized and demagnetized, but the essential detail is that the majority of soft magnetic materials such as magnetic nanoparticles, require no more than 0.5 Tesla to saturate or to be magnetized. The goal to bring VSM magnetic field to 0.5 Tesla, can be achieved based on the Faraday's Law of induction. For this thesis project, the challenge of increase the magnetic field (B) is going to be improve by adding transformers in order to increase the current and thus the magnetic field provided by the electromagnet. The dimensions of the air-gap, and also the surface of electromagnets are also important factors to consider when working on improving the magnetic field. The type of lamination shape of the magnetic core is also another important detail for the creation of the electromagnet. The final VSM electromagnet is shown in Figure 3.1.

### 3.1 Electromagnet

The construction of the electromagnet starts with the acquisition of two microwave transformer. Each transformer has a shell type construction and an "EI" core shape. The "E" core shape from each transformer was disassembled to form the new core for the VSM electromagnet. The central parts were beveled in order to concentrate the magnetic flux lines and thus increase the field in the air gap where the sample is going to be placed, Figure 3.2 shows a representation of the devised design. As mentioned in Chapter 2 section 2.3, the magnetic flux density is define as the number of magnetic flux lines per unit area passing through a plane perpendicular to the direction of the lines. Thus, the surface area of the electromagnets poles were reduce in order to achieve high values of magnetic field. The dimensions of the electromagnets poles are shown in Figure 3.7. The final electromagnet built is shown in Figure 3.1 and its scheme is shown in Figure 3.2.

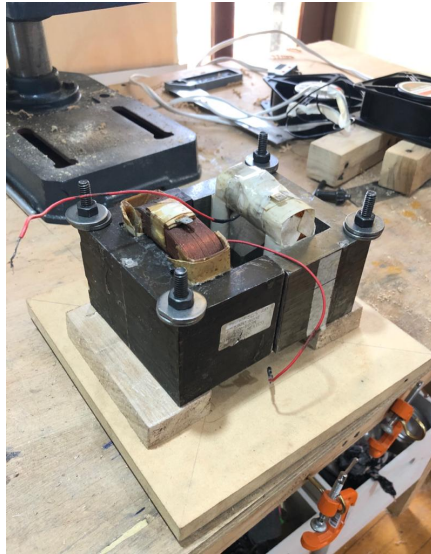


Figure 3.1: Picture of the final electromagnet built.

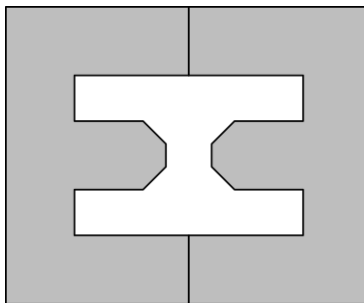


Figure 3.2: The disposition of the two "E" core shape design for the electromagnet final core.

## 3.2 Power supply

The power supply consist on nine transformers connected in series, a selector switch, the full-wave bridge rectifier, and a capacitor-input filter, as Figure 3.3. Each transformer consist in an output of three wires, 0-12-24 Volts, after the series connection, it is possible to increase the output voltage in step of 12 V. Eighteen switches are dispose in a circular selector that allow to increase the voltage up to 216 V. The circular selector was built in order to avoid confusion and a possible event of two or more switches chosen on. The detailed disposition of the voltage selector on the front panel of the power supply is shown in Figure 3.4. The maximum voltage of 216 V allows to circulate a current of 1.42 Ampere through the electromagnet coils creating a magnetic field of 0.5 Tesla.

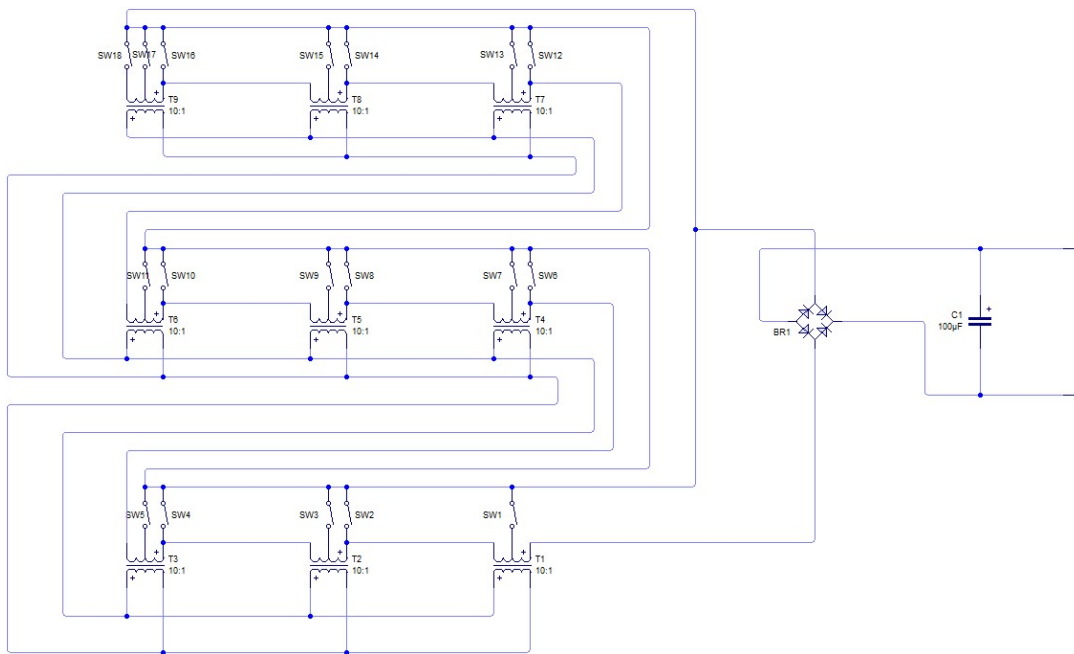


Figure 3.3: Transformer, rectifier and capacitor circuit.

The transformer coupling of the ac input voltage from the source to the rectifier is done with nine transformers. There exist two advantages from the transformer coupling: it allows the source voltage to be stepped down as needed, and the AC source is electrically isolated from the rectifier, thus prevent a shock hazard in the secondary circuit.<sup>28</sup>

The full-wave bridge rectifier converts the AC input voltage from the nine transformers to a pulsating DC voltage. Then, a capacitor-input filter eliminates the fluctuations in the rectified voltage and produces a relatively smooth DC voltage.<sup>28</sup> The electrical circuit connection is then formed by 9 transformers, full-wave bridge rectifier, and a capacitor-input filter. See Figure 3.3 The high voltage coils from each transformer played an important role to create a 0.5 Tesla magnetic field.

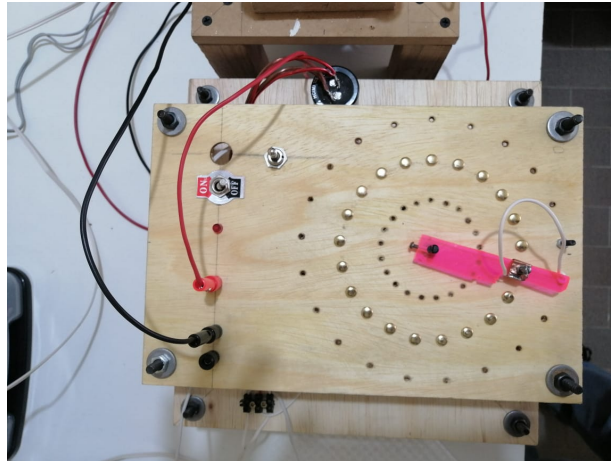


Figure 3.4: Front panel of the power supply. The selector switch consists of 20 paper sheet brass fasteners disposed in circular geometry (only 18 fasteners were connected).

### 3.3 Calibration

The calibration measurement starts with the improvement of the electromagnet magnetic field. The use of 3 transformers initially results in 170 mT, with a 73 volts consuming all system connected. Each transformer had an input of 300 mA current, AC 110V/220V voltage, and an output voltage AC 12 V, and 3 A. The electromagnets were polished and the surface area was measured again given a total area of  $3.51 \text{ cm}^2$  ( $2.7 \text{ cm} \times 1.3 \text{ cm}$ ) for one electromagnet pole and  $3.5 \text{ cm}^2$  ( $2.5 \text{ cm} \times 1.4 \text{ cm}$ ) for the other, see in Figure 3.6.

The 3 transformers were connected in series again, and the magnetic flux was measured in between the two electromagnets core where there is an air-gap 1.2 cm long, see in Figure 3.7. The magnetic flux measured 238 mT.

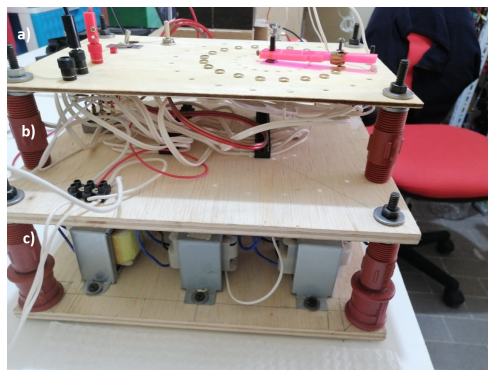


Figure 3.5: Configuration of the system: a) Selector switch, b) Diode bridge rectifier, c) Transformers.

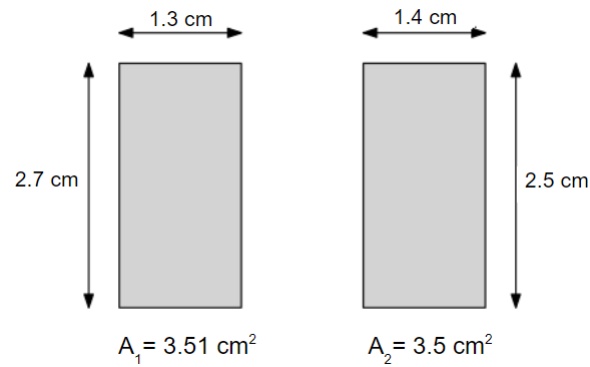


Figure 3.6: As the magnetic core of the two microwave transformer were beveled, the measurement of the dimensions from the two electromagnet poles were performed next: for the first electromagnet pole ( $A_1 = 2.7 \text{ cm} \times 1.3 \text{ cm} = 3.51 \text{ cm}^2$ ) and for the second electromagnet pole ( $A_2 = 2.5 \text{ cm} \times 1.4 \text{ cm} = 3.5 \text{ cm}^2$ ).

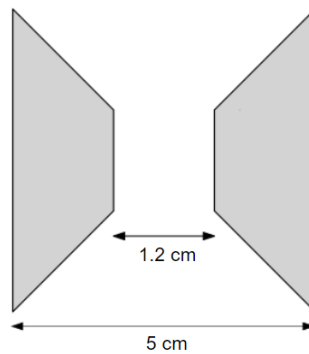


Figure 3.7: The measurement of the distance between the two electromagnet poles was performed; showing 1.2 cm for the inner gap where the sample is going to be placed and 5 cm for the distance between the complete electromagnet poles.

The current in the electromagnet gave 0.58 A, the voltage gave 103.3 V and the resistance 179 omhs. Calculations showed that 9 units of transformers are required in order to increase the electromagnet magnetic field approximately to 500 mT. Finally, 9 transformers were connected in series as the circuit shown in Figure 3.3. The use of a circular selector avoid two or more switches chosen on. The capacitor is use to filter the voltage, then a rectifier bridge is use to rectify the final voltage. The complete configuration system used for the calibration is shown in Figure 3.5.

### 3.3.1 Calibration Curve

The calibration of the electromagnet magnetic field was performed after the entire set up was connected as shown in Figure 3.9. A Gaussmeter tip was used in order to measure the magnetic field in between the electromagnet poles, see in Figure 3.10. The calibration curve is represented in Figure 3.8. The values of current in Amperes and magnetic flux density in milliTesla were collected. There are two types of measurement, the increase or up current and the decrease or down current.

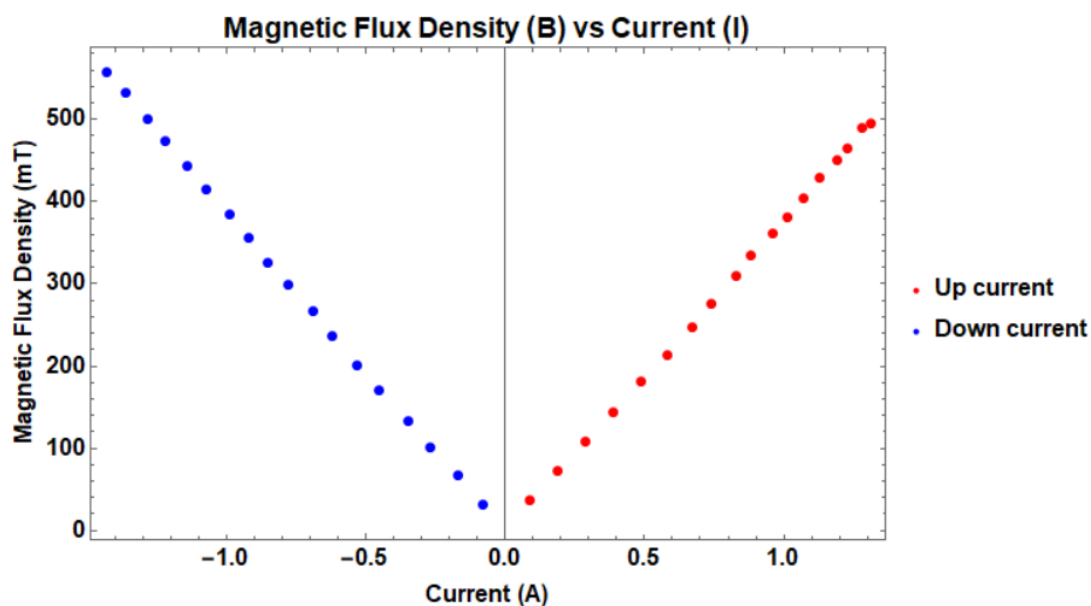


Figure 3.8: Flux density and current calibration curve. The red dots represent the up current where the measurement begins at 36 mT; 0.09 A and ends up at 496 mT; 1.31 A. The blue dots represent the down current where the measurement begins at 557 mT; 1.42 A and ends up at 32 mT; 0.08 A.

The up current measurement starts by using the selector switch to connect 1 output line from 1 transformer giving 36 mT and 0.09 A. Then, after using the selector switch to connect 18 output lines from 9 transformers in series, the final value was 496 mT and 1.31 A, see Figure 3.8 as the red dots. The down current measurement starts by using the selector switch to connect 18 output lines from 9 transformers in series, obtaining 557 mT and 1.42

A. Then, after using the selector switch to connect 1 output line from 1 transformer, the final value was 32 mT and 0.08 A, see Figure 3.8 as the blue dots. The difference between the two measurements of magnetic field values is due to the increase of temperature in the electromagnet core. Eddy currents are circular currents that flow within the electromagnet core. Based on Joule effect, the eddy currents trigger electrons to collide between each other and also with atoms of the material, as a consequence there is an increase of temperature in the magnetic core. The heat is transmitted to the coil wire and therefore its resistance tends to increase, thus for a specific voltage the current will be lower. Finally, the maximum magnetic field from the up current measurement is lower than 0.5 Tesla because the coil from the electromagnet core got hotter than 40 °C.

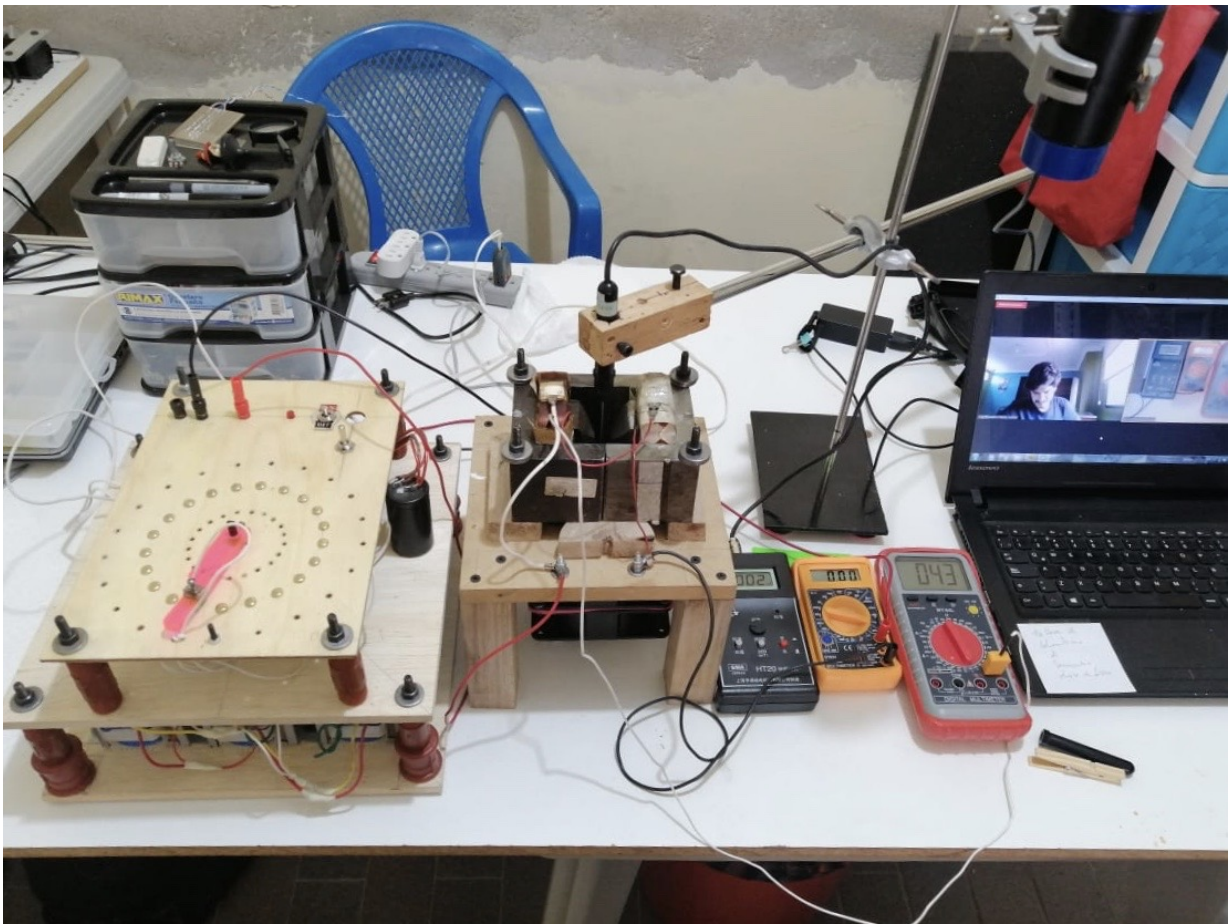


Figure 3.9: The entire setup connected to perform the calibration. The magnetic field is measured using a Gaussmeter, voltage and current are measured using two multi-meters.

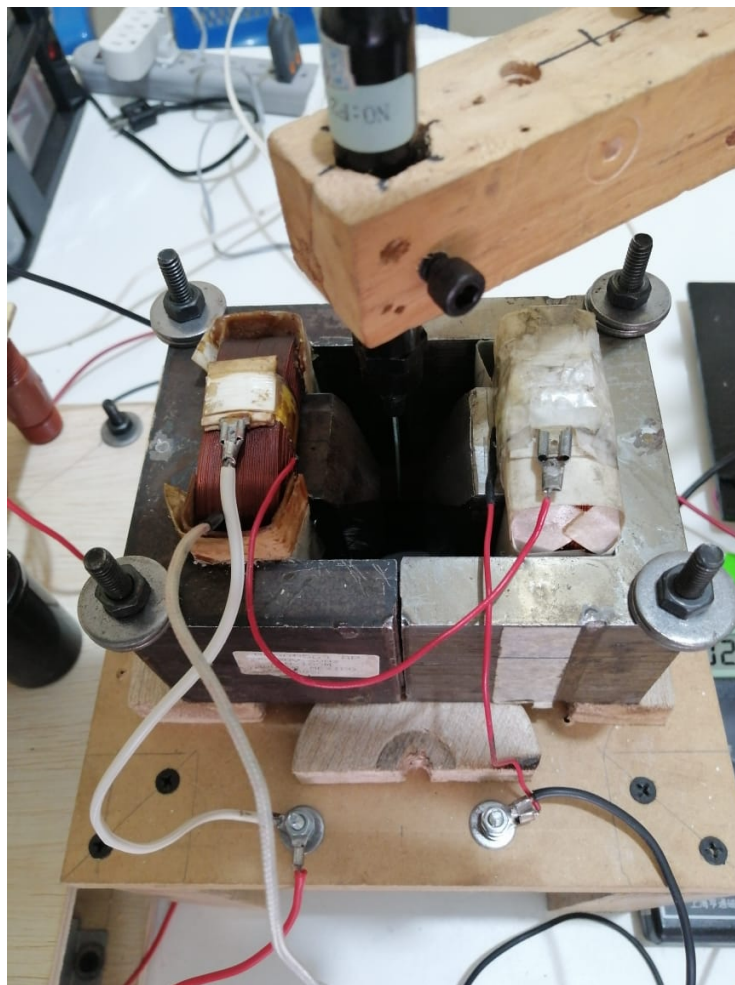


Figure 3.10: Detail of the electromagnet air gap with the Gaussmeter tip inside.

## Chapter 4

# Conclusions & Outlook

The VSM electromagnet core, managed to reach 0.5 Tesla after using 9 transformers connected in series. In addition, the design of the circuit that includes a full-wave bridge rectifier that converts the input AC signal to DC signal, a capacitor-input filter that eliminates the fluctuations in the rectified voltage. As a last step, a selector was used to prevent the transformers from being connected simultaneously. The 18 paper sheet brass fasteners provided the up current and down current shown in Figure 3.8 from Chapter 3.

The VSM technique would provide information about soft magnetic materials, including magnetic nanoparticles. There is a great number of applications using magnetic nanoparticles that can be described by using VSM. The goal of reaching 0.5 Tesla would bring the possibility to be used at undergraduate Yachay Tech laboratories.

For future research project, the improve of a refrigeration system could achieve better results for the develop of the VSM electromagnet core because overheating was found during the measurement of each value of magnetic flux density.



## Appendix A

# Magnetic Units Conversion

Magnetic Units Conversion					
	Reading	G	mT	Oe	kA/m
1G	Gauss	-	0.1	1	0.07977
1mT	milli Tesla	10	-	10	0.7977
1Oe	Oersted	1	0.1	-	0.07977
1kA/m	kilo Ampere per meter	12.54	1.254	12.54	-

Table A.1: Magnetic Units Conversion



## Appendix B

# Principal Units of Magnetism

In magnetism, there are currently three principal systems of units. The Gaussian or CGS system, the Sommerfeld and the Kennelly conventions. These systems of units have their advantages and disadvantages. The Gaussian system is based on magnetostatics and the concept of the magnetic pole. The SI system which is the Sommerfeld and the Kennelly, takes an electrodynamic approach to magnetism based on electric currents.<sup>22</sup>

Principal Units in Magnetism				
Quantity	Symbol	SI (Sommerfeld)	SI (Kennelly)	EMU(Gaussian)
Field Strength	H	$A \cdot m^{-1}$	$A \cdot m^{-1}$	oersteds
Flux Density	B	Tesla	Tesla	Gauss
Magnetization	M	$A \cdot m^{-1}$	-	emu/cc
Intensity of magnetization	I	-	Tesla	-
Flux	$\Phi$	Weber	Weber	Maxwell
Moment	m	$A \cdot m^2$	Weber meter	emu
Pole Strength	p	$A \cdot m$	Weber	emu/cm
Field Equation		$B = \mu_0 (H + M)$	$B = \mu_0 H + I$	$B = H + 4\pi M$
Energy on moment (free space)		$E = -\mu_0 m \cdot H$	$E = -m \cdot H$	$E = -m \cdot H$
Torque on moment (free space)		$\tau = \mu_0 m \times H$	$\tau = m \times H$	$\tau = m \times H$

Table B.1: Principal Units in Magnetism



# Bibliography

- [1] Marghussian, V. *Nano-Glass Ceramics*; 2015; pp 181–223.
- [2] Foner, S. Versatile and sensitive vibrating-sample magnetometer. *Review of Scientific Instruments* **1959**, *30*, 548–557.
- [3] Thomson, T. *Metallic Films for Electronic, Optical and Magnetic Applications: Structure, Processing and Properties*; Elsevier Ltd., 2013; pp 454–546.
- [4] Guachun, F. P.; Raposo, V. J. Diseño Y Calibración De Un Magnetómetro De Muestra Vibrante: Caracterización De Materiales Magnéticos. *Momento* **2018**, 45–62.
- [5] Rigue, J.; Chrischon, D.; De Andrade, A. M.; Carara, M. A torque magnetometer for thin films applications. *Journal of Magnetism and Magnetic Materials* **2012**, *324*, 1561–1564.
- [6] Adeyemi, N. *Faraday balance magnetometer*.
- [7] Alamdar, S.; Shah, H. Vibrating Sample Magnetometry : Analysis and. *Thesis* **2013**,
- [8] Magneto-optic Kerr effect - Wikiwand. [https://www.wikiwand.com/en/Magneto-optic\\_Kerr\\_effect](https://www.wikiwand.com/en/Magneto-optic_Kerr_effect).
- [9] Spintronics: Magneto-Optical Kerr Effect (MOKE) | Montana Instruments. <https://www.montanainstruments.com/Applications/Spintronics-Magneto-Optical-Kerr-Effect-MOKE/>.
- [10] Vanderbemden, P. *Design of an A.C. susceptometer based on a cryocooler*; Vol. 38; p 839.
- [11] Chen, K. L.; Chen, J. H.; Liao, S. H.; Chieh, J. J.; Horng, H. E.; Wang, L. M.; Yang, H. C. Magnetic clustering effect during the association of biofunctionalized magnetic nanoparticles with biomarkers. *PLoS ONE* **2015**, *10*.
- [12] Rosales Rivera, A.; Restrepo, J.; Sanin, M.; Patiño, O. Laboratorio de Magnetismo y Materiales Avanzados Universidad Nacional de Colombia Sede Manizales. *Revista Colombiana de Física* **2006**, *38*, 77–80.
- [13] Lopez-Dominguez, V.; Quesada, A.; Guzmán-Mínguez, J. C.; Moreno, L.; Lere, M.; Spottorno, J.; Giacomone, F.; Fernández, J. F.; Hernando, A.; García, M. A. A simple vibrating sample magnetometer for macroscopic samples. *Review of Scientific Instruments* **2018**, 89.

- [14] Department, S. P. *Vsm Principles*; 2006; pp 1–5.
- [15] Bowden, G. J. Detection coil systems for vibrating sample magnetometers. *Journal of Physics E: Scientific Instruments* **1972**, 5, 1115–1119.
- [16] Laboratory, B. Magnetic characterization of ferromagnetic samples by Vibrating Sample Magnetometry. *Materials Science and Engineering Vibrating* **2016**, 2–16.
- [17] Niazi, A.; Poddar, P.; Rastogi, A. K. A precision, low-cost vibrating sample magnetometer. *Current Science* **2000**, 79, 99–109.
- [18] Physics, H. Faraday's Law. <http://hyperphysics.phy-astr.gsu.edu/hbase/electric/farlaw.html>.
- [19] Lumen, Magnetic Flux, Induction, and Faraday's Law | Boundless Physics. <https://courses.lumenlearning.com/boundless-physics/chapter/magnetic-flux-induction-and-faradays-law/>.
- [20] Mcllyman, C. W. *Transformer and Inductor Design Handbook*; 2004.
- [21] Electronics, T. Electromagnetism and Electricity for Electromagnets. <https://www.electronics-tutorials.ws/electromagnetism/electromagnetism.html>.
- [22] Jiles, D. *Introduction to Magnetism and Magnetic Materials*; Springer US, 1991.
- [23] Zureks, File:Permeability by Zureks.svg - Wikimedia Commons. <https://commons.wikimedia.org/w/index.php?curid=6577080>.
- [24] Byjus, Magnetic Permeability -Definition, Formula, Units, Types. <https://byjus.com/jee/magnetic-permeability/>.
- [25] Dekker, M. *Chapter 2 Magnetic Materials and Their Characteristics*; 2004.
- [26] Wikibooks, A-level Physics (Advancing Physics)/Transformers - Wikibooks, open books for an open world. [https://en.wikibooks.org/wiki/A-level\\_Physics\\_\(Advancing\\_Physics\)/Transformers](https://en.wikibooks.org/wiki/A-level_Physics_(Advancing_Physics)/Transformers).
- [27] Physics, H. Transformer. <http://hyperphysics.phy-astr.gsu.edu/hbase/magnetic/transf.html#c1>.
- [28] Gayler, J.; Titus, K. J.; Clapp, T. G. *Textile Horizons*; 1997; Vol. 17; pp 16–20.
- [29] Venäläinen, A. Modification of bare and functionalized Au(111) surfaces and ferromagnetism of Au and Pd nanoclusters. Ph.D. thesis, 2018.
- [30] Byjus, Paramagnetic Materials - Definition, Examples, Properties. <https://byjus.com/jee/paramagnetic-materials/>.

- [31] Britannica, Electromotive force | physics | Britannica. <https://www.britannica.com/science/electromotive-force>.
- [32] Britannica, Ferrimagnetism | physics | Britannica. <https://www.britannica.com/science/ferrimagnetism>.
- [33] Byjus, Ferromagnetic Materials - Definition, Causes of Ferromagnetism, Examples, Uses. <https://byjus.com/jee/ferromagnetic-materials/>.
- [34] Enriquez-Navas, P. M.; Garcia-Martin, M. L. *Frontiers of Nanoscience*; Elsevier Ltd, 2012; Vol. 4; pp 233–245.
- [35] Steinmetz, C. File:Magnetization curves.svg - Wikimedia Commons. [https://commons.wikimedia.org/wiki/File:Magnetization\\_curves.svg](https://commons.wikimedia.org/wiki/File:Magnetization_curves.svg).
- [36] Hamakawa, *United States Patent (19) Hamakawa et al. (54) THIN FILM MAGNETIC HEAD HAVING AT LEAST ONE MAGNETIC CORE MEMBER MADE AT LEAST PARTLY OF A MATERIAL HAVING A HIGH SATURATION MAGNETIC FLUX DENSITY*; 1990.
- [37] Magnetics, K. Shielding Materials. <http://www.kjmagnetics.com/blog.asp?p=shielding-materials>.
- [38] Hu, B.; He, M.; Chen, B. *Solid-Phase Extraction*; Elsevier Inc., 2019; pp 235–284.
- [39] Zureks, File:B-H loop.png - Wikimedia Commons. [https://commons.wikimedia.org/wiki/File:B-H\\_loop.png](https://commons.wikimedia.org/wiki/File:B-H_loop.png).
- [40] Darling, D. Hysteresis loop by Internet Encyclopedia of Science. 2016; [http://sciencewise.info/resource/hysteresis\\_loop/Hysteresis\\_loop\\_by\\_Internet\\_Encyclopedia\\_of\\_Science](http://sciencewise.info/resource/hysteresis_loop/Hysteresis_loop_by_Internet_Encyclopedia_of_Science).
- [41] Birmingham, *Magnetic Materials: Soft Magnets*.
- [42] García, M. C.; Uberman, P. M. *Nanocarriers for Drug Delivery*; 2019; pp 43–79.



# Abbreviations

**EMF** Electromotive force 9

**MNPs** Magnetic Nanoparticles 22

**VSM** Vibrating Sample Magnetometer 1